Available online at www.sciencedirect.com
ScienceDirect
Trans. Nonferrous Met. Soc. China 21(2011) 2568−2575
Transactions of Nonferrous Metals Society of China
www.tnmsc.cn

Fracture strength of centre surface cracked tensile specimens made of 2219-T87 Al alloy welding

S. RAJAKUMAR[1], T. CHRISTOPHER[2]

1. Thanthai Periyar Government Institute of Technology, Vellore-632002, India;
2. Government College of Engineering, Perumalpuram, Tirunelveli-627007, India

Received 21 March 2011; accepted 8 June 2011

Abstract: Fracture data of both parent metal and weldment metals from surface cracked tensile plates made of 2219-T87 Al alloy at cryogenic temperatures were correlated using a modified inherent flaw model. Fracture parameters to generate the failure assessment diagram were determined for the material. Fracture analysis was carried out considering the ultimate tensile strength value and the fracture data of aluminium base metal and weldment metal generated from center–surface cracked tensile specimens having different thicknesses. The failure assessment diagram of a material generated from tensile fracture plate configuration can be applied to failure pressure estimation of any cracked component, made of the same material.

Key words: centre through crack; tensile specimen; failure assessment diagram; fracture strength; inherent flaw model; 2219-T87 Al alloy

1 Introduction

Damage tolerant and fail-safe approaches have been employed increasingly in the design of critical engineering components. In these approaches, one has to assess the residual strength of a component with an assumed pre-existing crack. In other cases, cracks may be detected during service. Then, there is a need to evaluate the residual strength of the cracked components in order to decide whether they can be continued safely or repair and replacement are imperative. When dealing with a specific material for a particular application, it is not clearly established whether K_{IC} (plane strain fracture toughness) or K_C (fracture toughness when plane strain conditions are not met) values should be used. The values of K_{IC} seem to be relevant in heavy sections like forgings or thick plates. Design based on K_{IC} requires unreasonably thick panels in normally thin-sectioned structural members in aerospace industry.

In such circumstances it is necessary to carry out what is called K_C tests as per ASTM-E561 standards, corresponding to the thickness of the members in the intended structural applications. The geometry dependent values of K_C can be determined from the point of tangency between the crack growth resistance curve (R-curve) and the crack driving force curve of a through-cracked configuration. For part through cracked configuration, fracture strength estimations are not possible directly from the R-curve of the material because the part through crack has two dimensions, namely, crack length and its depth.

The significant parameters affecting the size of a critical crack in a structure are the applied stress levels, the fracture toughness of the material, the location of the crack and its orientations. Since the intensity of the stress at the crack tip, K, is a function of load, geometry and crack size, it is more appropriate to have a relationship between the stress intensity factor at failure (K_{max}) and the failure stress (σ_f) from the fracture data of cracked specimens for the estimation/prediction of the fracture strength to any cracked configuration. For cracked configurations, a relation between the stress intensity factor (K_{max}) and the corresponding stress (σ_f) at failure is suggested as [1−4]:

$$K_{\max} = K_F\left\{1 - m\left(\frac{\sigma_f}{\sigma_u}\right) - (1-m)\left(\frac{\sigma_f}{\sigma_u}\right)^p\right\} \quad (1)$$

where σ_f is the failure stress normal to the direction of

Corresponding author: S. RAJAKUMAR; E-mail: s_rajakumar59@yahoo.co.in
DOI: 10.1016/S1003-6326(11)61093-5

the crack in a body and σ_u is the nominal stress required to produce a plastic hinge on the net section. For the pressurized cylinders, σ_f is the hoop stress at the failure pressure of the flawed cylinder, and σ_u is the hoop stress at the failure pressure of an unflawed cylinder. For the determination of three fracture parameters (K_F, m and p), test results of simple laboratory specimens like compact tension specimens, center crack specimens etc, can be utilized. For fracture strength evaluation of any other structural configuration, the stress intensity factor corresponding to that geometry is used in Eq. (1) to develop the necessary fracture strength equation. If the values of applied stress and corresponding stress intensity factor for the specified crack size in a structure lie below the K_{max}—σ_f curve of the failure assessment diagram, the structure for that loading condition is safe.

Fracture data [5] have been obtained for 2219-T87 Al alloy useful for aircraft applications. The objective of this work is to utilize an improved inherent flaw model for tensile fracture strength evaluation of 2219-T87 Al alloy.

2 Modified inherent flaw model

The stress intensity factor for a wide tensile specimen having a centre crack is expressed as

$$K_I = \sigma\sqrt{\pi c} \tag{2a}$$

where σ is the applied stress and c is the half crack length. Similar to Irwin's plastic zone correction, the assumption of the existence of an intense energy region of length a_{ci} (Fig. 1) results in the following equation for a wide centre crack tensile specimen at failure:

$$K_{Q\infty} = \sigma_{NC}^{\infty}\sqrt{\pi(c + a_{ci})} \tag{2b}$$

were σ_{NC}^{∞} is the fracture strength of the wide tensile specimen having a centre crack of length $2c$; a_{ci} is the crack-tip damage size at failure. In other words, (c+a_{ci}) is an effective half crack length. In the case of unflawed specimens, the fracture strength equals the ultimate tensile strength (σ_o) and Eq. (2b) becomes

$$K_{Q\infty} = \sigma_0\sqrt{\pi a_{ci}} \tag{2c}$$

Thus, a_{ci} can be considered equivalent to the half crack length of an inherent flaw in the unflawed tensile specimen. Accordingly, this model is known as "the inherent flaw model (IFM)"or "the WEK model" [6].

From Eqs. (2b) and (2c), one can express

$$\sigma_{NC}^{\infty} = \frac{\sigma_0}{\sqrt{\dfrac{c}{a_{ci}} + 1}} \tag{3}$$

The unknown characteristic length (a_{ci}) is obtained from the test data of a finite width tensile cracked specimen. The fracture strength (σ_{NC}^{∞}) of the center crack wide tensile specimen is obtained from that of a finite width specimen (σ_{NC}) as

$$\sigma_{NC}^{\infty} = \sigma_{NC} Y \tag{4}$$

where the finite width correction factor [7], Y, is

$$Y = \sqrt{\sec\left(\frac{\pi c}{W}\right)} \tag{5}$$

where W is the specimen width.

Using σ_{NC}^{∞}, σ_0 and c, the unknown characteristic a_{ci} is found from Eq. (3) as

$$a_{ci} = \frac{c}{\left(\dfrac{\sigma_0}{\sigma_{NC}^{\infty}}\right)^2 - 1} \tag{6}$$

Knowing the characteristic length (a_{ci}), Eq. (3) gives the fracture strength (σ_{NC}^{∞}) for the specified crack length ($2c$). Fracture strength (σ_{NC}) of the finite width plate is obtained from Eq. (4) or by dividing (σ_{NC}^{∞}) with the correction factor (Y). It is well known that the fracture strength decreases with the increase in the crack size. Equation (6) indicates that the characteristic length (a_{ci}) need not be a material constant. This calls for a modification in the inherent flaw model.

A relation between (a_{ci}) and (σ_{NC}^{∞}) in the non-dimensional form is proposed as

$$\frac{\sigma_0\sqrt{\pi a_{ci}}}{K_{IFM}} = 1 - \delta_{aci}\frac{\sigma_{NC}^{\infty}}{\sigma_0} \tag{7}$$

To determine the parameters (K_{IFM} and δ_{aci}) in Eq. (7), two cracked specimen tests in addition to an unflawed specimen test are required. Normally, more tests are performed to take into account of the scatter in test results. The parameters K_{IFM} and δ_{aci} in Eq. (7) are

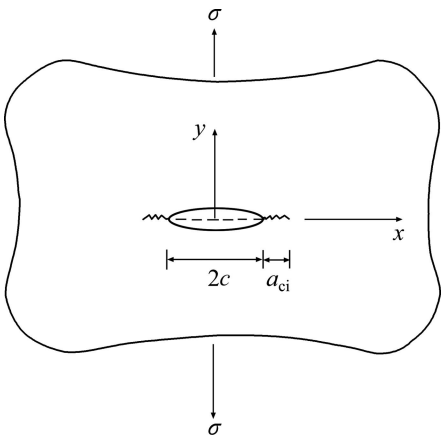

Fig. 1 Characteristic length (a_{ci}) in a center-crack wide tensile panel

determined by a least square curve fit to the data for a_{ci} and $\sigma_{NC}^{\infty}/\sigma_0$. Using Eqs. (6) and (7), one can write the following nonlinear equation for the fracture strength (σ_{NC}^{∞}) after eliminating the characteristic length (a_{ci}) as

$$\frac{1}{\pi}\left(\frac{K_{IFM}}{\sigma_{NC}^{\infty}}\right)^2\left[1-\delta_{aci}\left(\frac{\sigma_{NC}^{\infty}}{\sigma_0}\right)\right]^2\left[1-\left(\frac{\sigma_{NC}^{\infty}}{\sigma_0}\right)^2\right]=C \quad (8)$$

This non-linear fracture strength equation (8) is solved using the Newton–Raphson iterative scheme to obtain (σ_{NC}^{∞}) for the specified crack size. The fracture strength σ_{NC}^{∞} versus crack size $2c$ curves can be generated from Eq. (8) by specifying $0<\sigma_{NC}^{\infty}<\sigma_0$ useful for evaluation of σ_{NC}^{∞} to any specific crack size. Applying the correction factor Y to σ_{NC}^{∞}, the fracture strength (σ_{NC}) can be found. A relationship between $K_Q(\equiv\sigma_{NC}^{\infty}\sqrt{\pi c})$ and $\sigma_{NC}^{\infty}/\sigma_0$ is obtained from Eq. (8) as

$$K_Q=K_{IFM}\left[1-\delta_{aci}\left(\frac{\sigma_{NC}^{\infty}}{\sigma_0}\right)\right]\sqrt{1-\left(\frac{\sigma_{NC}^{\infty}}{\sigma_0}\right)^2} \quad (9)$$

Equation (9) represents a failure assessment diagram useful for fracture strength evaluation of different cracked configurations.

3 Equivalent through crack

The procedure proposed above is highly convenient for equivalent through cracked specimens. However, for part-through cracks (Fig. 2), the definition of inherent flaw is not straight forward. Hence, an attempt is made to evaluate equivalent through crack size for the given part-through cracked size.

To establish fracture strength of a structural component in the presence of a crack, the stress intensity

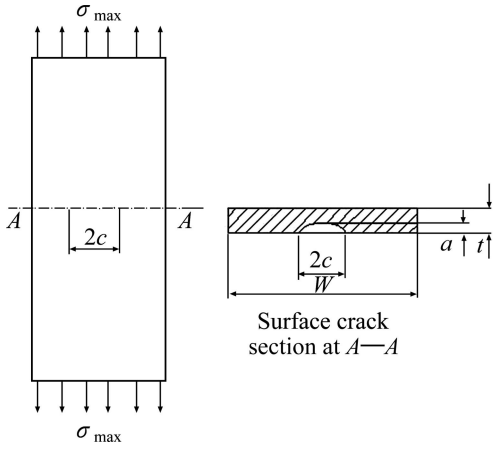

Fig. 2 Centre surface cracked plate subjected to a uniform tensile stress σ_{max}

factor corresponding to that cracked body is essential to setup a fracture strength equation. The stress intensity factor K_{max} for centre surface crack tension (SCT) specimens from the stress intensity factor expressions obtained from finite element solutions [8−9] are

$$K_{max}=\sigma_f(\pi a)^{1/2}M\phi$$

where $\sigma_f=\sigma_{max}$ for SCT specimens;

$$M=\left[M_1+\left(\phi\sqrt{\frac{c}{a}}-M_1\right)\left(\frac{a}{t}\right)^{\sqrt{\pi}}+\phi\sqrt{\frac{c}{a}}(M_2-1)\left(\frac{a}{t}\right)^{2\sqrt{\pi}}\right]f_w$$

for SCT specimens;

$\phi^2=1+1.464(a/c)^{1.65}$, for $a\le c$;

$\phi^2=1+1.464(c/a)^{1.65}$, for $a>c$;

$M_1=1.13-0.1(a/c)$, for $a\le c$;

$$M_1=\left[1+0.03\left(\frac{c}{a}\right)\right]\left(\frac{c}{a}\right)^{1/2},\ \text{for } a>c;$$

$$M_2=\left(\frac{\pi}{4}\right)^{1/2},\ \text{for } a\le c;$$

$$M_2=1+\left(\frac{c}{a}\right)\left[\left(\frac{\pi}{4}\right)^{1/2}-1\right],\ \text{for } a>c;$$

$$f_w=\sqrt{\sec\left[\left(\frac{\pi c}{w}\right)\left(\frac{a}{t}\right)^{1/2}\right]}$$

where a is the depth and c is half the crack length of a surface crack and w is the width of the plate. When $a=t$, the expression holds good for through crack. From the given test data [5], first K_{max} is calculated for surface crack. Then, using the same K_{max} and assuming $a=t$, the equivalent through crack length $2c_{eq}$ can be calculated using Newton–Raphson iterative process. The calculated $2c_{eq}$ is used in IFM. A Nomogram is given to find out $2c_{eq}$ from $2c$.

4 Results and discussion

The fracture data [5] of 2219-T87 Al alloy useful for aircraft applications is utilized in the present study to verify the validity of the fracture criterion. The unnotched strength (σ_0) data in Table 1 are categorized by material and temperature. The average strength value of the multiple test results is considered in the analysis.

Fracture analysis has been carried out considering the ultimate tensile strength values and the fracture data of aluminium base metal and weldment metal generated

from center−surface crack tensile specimens having different thicknesses. From the fracture strength (σ_{NC}) data of the finite width center-crack tension specimens, the fracture strength (σ_{NC}^{∞}) for wide tensile specimens is obtained from Eq. (4). Substituting the crack length ($2c$), the unnotched strength (σ_0) and the notched strength (σ_{NC}^{∞}) in to Eq. (6), the characteristic length (a_{ci}) is obtained. The values of a_{ci}, σ_{NC}^{∞} and σ_0 from fracture data are fitted in Eq. (7) to obtain the fracture parameters (K_{IFM} and δ_{aci}). Table 1 gives the determined fracture parameters (K_{IFM} and δ_{aci}) from the test data of aluminium alloy. One can generate fracture strength (σ_{NC}^{∞}) versus the crack size ($2c$) curves from Eq. (8) by specifying the values of σ_{NC}^{∞} from 0 to σ_0. From this curve, one can find easily the fracture strength (σ_{NC}^{∞}) for the crack size. Then, applying the finite width correction factor (Y) to σ_{NC}^{∞}, the fracture strength (σ_{NC}) for the finite width plate can be estimated. In the present study, the non-linear fracture strength from Eq. (8) is solved using the Newton-Raphson iterative method.

Tables 2 to 4 give the comparison of fracture strength estimations with the test results for 2219-T87 base metal at temperatures of 295, 77, and 20 K, respectively, for t=16 mm. Tables 5 to 7 give the comparison of fracture strength estimations with the test results for 2219-T87 weldment metal at temperatures 295, 77, and 20 K, respectively, for t=25 mm. Tables 8 and 9 give the comparison of fracture strength estimations with the test result for 2219-T87 weldment metal at temperature 295 and 77 K for t=3 mm. The standard error is found to be less than 0.1, which indicates that the fracture strength estimations utilizing the fracture parameters (K_{IFM} and δ_{aci}) can be expected within ±10% of the test results. Figures 3 and 4 show the failure assessment diagrams including the fracture data [5] of the materials for 2219-T87 base metal at temperatures 77 and 295 K, respectively, for t=16 mm. Figures 5 and 6 show the failure assessment diagrams including the fracture data [5] of the materials for aluminium 2219-T87 weld metal at 77 and 20 K, for t=25 mm. Figures 3 to 6 indicate the

Table 1 Fracture parameters (K_{IFM} and δ_{aci}) evaluated from test results [5] of centre surface crack tension specimens made of 2219-T87Al alloy

Alloy specification	Temperature/K	Un-notched strength/MPa	Specimen thickness/mm	N*	Fracture parameter in Eq. (8)	
					K_{IFM}/(MPa·m$^{1/2}$)	δ_{aci}
2219−T87 base metal	295	477.1	16.0	7	79.28	0.00
	77	592.3	16.0	25	74.52	0.00
	20	646.8	16.0	16	76.5	0.00
2219−T87 base metal	295	468.17	1.7	14	69.95	0.00
	77	583.32	1.7	12	124.61	0.53
	20	647.44	1.7	12	156.63	0.75
2219−T87 weldment metal	295	263.4	25.0	7	140.02	0.93
	77	379.2	25.0	5	54.08	0.00
	20	433.0	25.0	6	41.25	0.00
2219−T87 weldment metal	295	263.4	3.0	4	125.63	1.00
	77	379.2	3.0	7	125.00	1.00
	20	433	3.0	5	45.29	0.00

* N−Number of specimens.

Table 2 Comparison between experimental and analytical fracture strength values for 2219-T87 base metal with σ_0=477.1 MPa, t=16 mm at temperature of 295 K (K_{IFM}=79.28 MPa·m$^{1/2}$, δ_{aci}=0)

Specimen dimension/mm					Fracture strength, σ_{NC}/MPa		Relative error/%
Width, W	Thickness, t	Crack depth, a	Crack length, $2c$	Equivalent crack length, $2c_{eq}$	Test [5]	Analysis	
228.5	16.3	7.52	61	30.5	291	285.2	2
558.9	16.3	15.24	145.41	133.3	148.9	156.9	−5.4
139.8	15.9	6.88	16.61	11.1	373	371.6	0.4
171.4	16.3	6.07	15.27	9.8	379.2	380.9	−0.5
139.7	16.3	8.61	23.42	16.7	331	338.4	−2.2
139.8	15.9	9.19	24.41	18	335.1	331.5	1.1
171.4	15.9	9.91	29.21	22.2	323.4	313.6	3

Standard error =0.026

Table 3 Comparison between experimental and analytical fracture strength values for 2219-T87 base metal with σ_0=592.3 MPa, t=16 mm at temperature of 77 K (K_{IFM}=74.52 MPa·m$^{1/2}$, δ_{aci}=0)

Specimen dimension/mm					Fracture strength, σ_{NC}/MPa		Relative error/%
Width, W	Thickness, t	Crack depth, a	Crack length, 2c	Equivalent crack length, 2c_{eq}	Test [5]	Analysis	
228.5	16.26	6.98	61.72	28.5	314.4	299.7	4.7
228.09	16.21	6.91	62.2	28.3	306.1	300.2	1.9
279.48	16.43	9.52	91.82	51.1	245.5	235.1	4.2
367.94	16.08	11.43	117.09	78	193.8	194.5	−0.4
558.9	16.33	13.33	137.29	105.7	148.2	170.7	−15.1
558.65	15.93	14.22	147.7	127.4	160.6	155	3.5
558.67	16.33	14.1	140.33	116.3	146.9	162.6	−10.7
139.62	16.33	6.27	24.66	15	391	372.7	4.7
139.67	16.03	6.65	24.84	15.6	393	367.7	6.5
228.68	16.21	8.92	33.1	23.1	314.4	324.1	−3.1
228.78	15.87	8.81	33.63	23.4	350.2	322.4	8
304.9	16.31	11.94	44.45	35.9	247.5	274.7	−11
304.88	16.08	12.19	45.21	37.3	275.8	270.4	2
305.03	15.9	14.35	52.58	48.8	237.9	241	−1.3
304.95	16.41	14.1	51.56	46.2	217.2	246.8	−13.6
139.7	16.43	6.32	15.54	10.1	424	416.9	1.7
139.62	16	5.71	14.91	9.5	422	423.3	−0.3
139.65	16.28	7.9	22.58	15.6	368.2	368.2	0
139.75	16.18	9.37	24.49	18.1	351	350.1	0.2
154.3	16.41	10.97	29.72	23.4	315.8	319.8	−1.3
171.4	16.05	10.59	29.59	23.1	339.9	322.2	5.2
171.45	16.05	12.34	34.62	29.4	303.4	293.7	3.2
171.53	16	11.99	34.8	29.1	305.5	294.9	3.4
304.57	16.31	13.87	34.82	31.3	260.6	289.9	−11.2
304.88	15.9	14.07	35.66	32.9	280.6	284.4	−1.3

Standard error =0.064

Table 4 Comparison between experimental and analytical fracture strength values for 2219-T87 base metal with σ_0=646.8 MPa, t=16 mm at temperature of 20 K (K_{IFM}=76.4 MPa·m$^{1/2}$, δ_{aci}=0)

Specimen dimension/mm					Fracture strength, σ_{NC}/MPa		Relative error/%
Width, W	Thickness, t	Crack depth, a	Crack length, 2c	Equivalent crack length, 2c_{eq}	Test [5]	Analysis	
228.6	16.26	5.71	61.59	22.9	342.7	339.7	0.9
228.5	16.33	5.79	61.72	23.2	342	338	1.2
279.6	16	9.52	91.31	52.1	233.1	241.5	−3.6
279.53	16	9.02	91.69	48.9	237.9	248.7	−4.5
367.97	16.31	11.68	118.62	79.9	184.1	198.7	−7.9
367.97	16.28	11.68	117.98	79.7	180	198.9	−10.5
368.02	16.28	12.7	136.52	101.1	162	175.2	−8.1
367.89	16.33	13.21	139.95	108.6	161.3	168.3	−4.3
139.7	16.38	5.69	15.01	9.5	464.7	448	3.6
139.45	15.85	5.49	14.96	9.5	473.7	448.7	5.3
139.62	16.43	9.02	24.28	17.6	377.2	371.1	1.6
139.6	15.87	8.94	23.62	17.3	392.3	373.3	4.8
171.4	16.28	10.72	29.87	23.3	344.1	335.6	2.5
171.45	16.08	10.41	29.49	22.8	353	338.5	4.1
171.37	16.31	12.09	34.57	28.7	305.5	309	−1.2
171.32	15.93	12.09	34.82	29.3	308.9	306.4	0.8

Standard error=0.049

Table 5 Comparison between experimental and analytical fracture strength values for 2219-T87 weldment metal with σ_0=263.4 MPa, t=26 mm at temperature of 295 K (K_{IFM}=140.023 MPa·m$^{1/2}$, δ_{aci}=0.934 4)

Specimen dimension/mm					Fracture strength, σ_{NC}/MPa		Relative error/%
Width, W	Thickness, t	Crack depth, a	Crack length, 2c	Equivalent crack length, 2c_{eq}	Test [5]	Analysis	
609.6	26	17.53	105.54	74.4	157.2	151.3	3.8
761.7	25.8	18.41	126.87	90.5	142.7	145.8	−2.2
762	26.2	21.46	150.24	121.8	140.7	136.2	3.1
342.9	25.6	17.68	60.38	47.6	162	163.1	−0.7
406.9	25.5	19.63	64.34	54.1	159.3	159.8	−0.4
406.7	25.5	21.08	72.39	63.4	152.4	154.8	−1.6
406.7	25.5	22.58	76.45	70.2	148.2	151.5	−2.2

Standard error =0.023

Table 6 Comparison between experimental and analytical fracture strength values for 2219-T87 weldment metal with σ_0= 379.2 MPa, t=26 mm at temperature of 77 K (K_{IFM}=54.079 MPa·m$^{1/2}$, δ_{aci}=0)

Specimen dimension/mm					Fracture strength, σ_{NC}/MPa		Relative error/%
Width, W	Thickness, t	Crack depth, a	Crack length, 2c	Equivalent crack length, 2c_{eq}	Test [5]	Analysis	
507.3	25.6	11.86	84.58	44.4	169.6	179.1	−5.6
609.7	25.9	18.03	107.82	78	136.5	141.4	−3.6
342.6	25.6	17.86	60.3	47.9	174.4	172.6	1.1
406.7	20.0	19.99	65.63	65.6	148.9	151.3	−1.6
406.4	25.6	21.36	71.93	63.5	168.2	153.5	8.8

Standard error =0.05

Table 7 Comparison between experimental and analytical fracture strength values for 2219-T87 weldment metal with σ_0=433 MPa, t=25 mm at temperature of 20 K (K_{IFM}=41.251 MPa·m$^{1/2}$, δ_{aci}=0)

Specimen dimension/mm					Fracture strength, σ_{NC}/MPa		Relative error/%
Width, W	Thickness, t	Crack depth, a	Crack length, 2c	Equivalent crack length, 2c_{eq}	Test [5]	Analysis	
508.2	25.6	15.75	105.79	67.8	119.3	119.7	−0.4
762	25.6	21.34	151.64	124.6	80	89.5	−11.9
342.2	25.8	18.03	59.31	47.3	139.3	140.9	−1.2
406.7	25.6	19.68	63.25	53.2	142.7	133.8	6.3
406.4	25.4	21.21	73.53	64.9	129.6	121.6	6.2
406.6	25.4	22.1	75.82	68.8	117.2	118.2	−0.8

Standard error =0.06

Table 8 Comparison between experimental and analytical fracture strength values for 2219-T87 weldment metal with σ_0=263.4 MPa, t=3 mm at temperature of 295 K (K_{IFM}=125.634 MPa·m$^{1/2}$, δ_{aci}=1.00)

Specimen dimension/mm					Fracture strength, σ_{NC}/MPa		Relative error/%
Width, W	Thickness, t	Crack depth, a	Crack length, 2c	Equivalent crack length, 2c_{eq}	Test [5]	Analysis	
152.8	3.1	1.42	22.64	8	226.2	194.6	14
95.3	3.2	1.19	8.66	4.1	218.6	206.8	5.4
95.3	3.1	1.6	12.6	6.7	204.1	197.7	3.1
95.3	3.1	2.08	15.98	10.6	209.6	188.1	10.3

Standard error =0.092

Table 9 Comparison between experimental and analytical fracture strength values for 2219-T87 weldment metal with σ_0=379.2 MPa, t=3 mm at temperature of 77 K (K_{IFM}=125 MPa·m$^{1/2}$, δ_{aci}= 1.00)

Specimen dimension/mm					Fracture strength, σ_{NC}/MPa		Relative error/%
Width, W	Thickness, t	Crack depth, a	Crack length, 2c	Equivalent crack length, 2c_{eq}	Test [5]	Analysis	
152.5	3.1	1.12	24.94	6	251.7	267.3	−6.2
190.7	3.1	2.21	35.56	21.2	237.9	222.9	6.3
241.6	3.1	2.06	47.37	22.9	228.9	220.5	3.7
95.3	3.1	1.17	8.74	4	275.1	278.8	−1.3
95.3	3.1	1.98	12.4	8.3	248.9	256.4	−3
95.2	3.1	2.18	16.03	11.1	237.2	245.7	−3.6
95.2	3.2	2.39	18.97	13.9	229.6	236.8	−3.2

Standard error =0.042

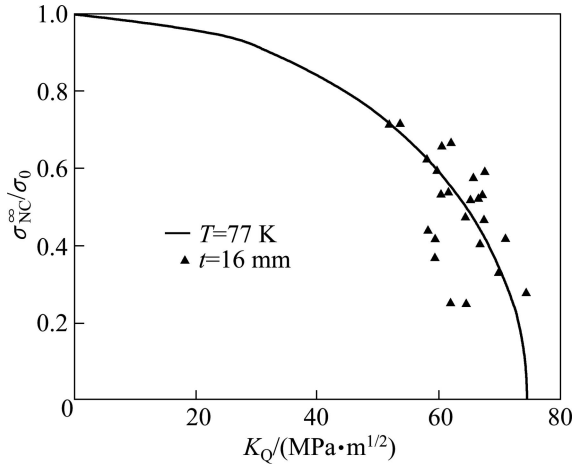

Fig. 3 Failure assessment diagrams for 2219-T87 base metal with test data [5] (K_{IFM}= 74.52 MPa·m$^{1/2}$, δ_{aci}=0)

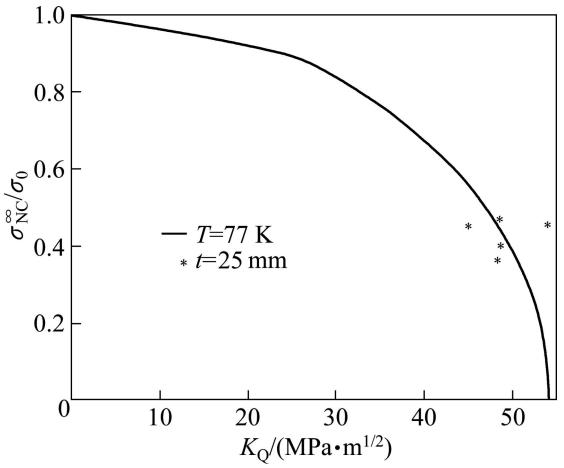

Fig. 5 Failure assessment diagrams for 2219-T87 weldment metal with test data [5] (K_{IFM}=54.08 MPa·m$^{1/2}$, δ_{aci} =0)

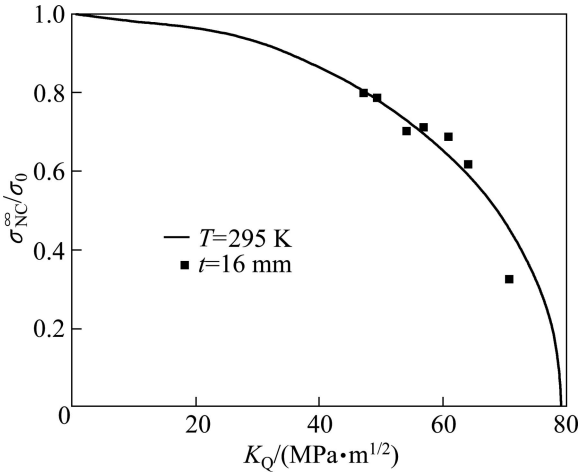

Fig. 4 Failure assessment diagrams for 2219-T87 base metal with test data [5] (K_{IFM}= 79.28 M Pa·m$^{1/2}$, δ_{aci}=0)

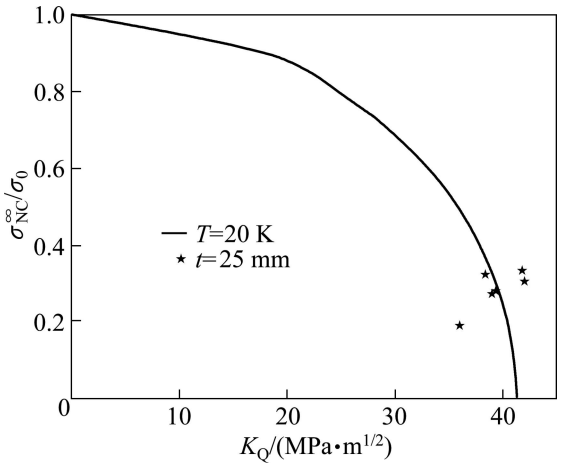

Fig. 6 Failure assessment diagrams for 2219-T87 weldment metal with test data [5] (K_{IFM}=41.25 MPa·m$^{1/2}$, δ_{aci} =0)

closeness with which the fracture data have been correlated using the modified inherent flaw model. One can use these failure assessment diagrams as a ready reference chart to verify whether the design point is in a safe region or not. If the specimen or the structure is with surface crack, a plot shown in Fig. 7 can be used to find equivalent through crack size, which may be used to find the fracture strength or design point from Figs. 3 to 6. It can be seen from Fig. 8 that most of the fracture strength estimations are within ±10% of the test results.

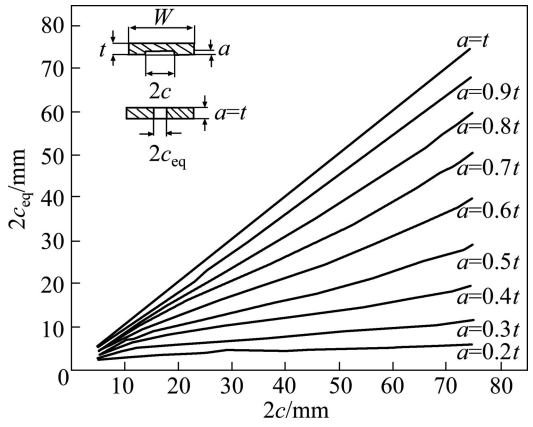

Fig. 7 Surface crack length versus equivalent through crack length

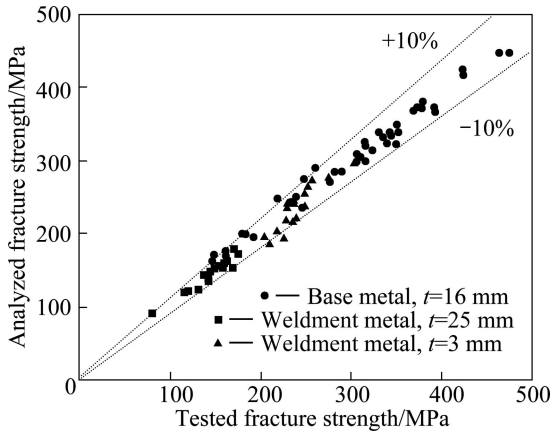

Fig. 8 Comparison of fracture strength of 2219-T87 Al alloy

5 Conclusions

The procedure was validated considering the fracture data of 2219-T87 Al alloy of center surface crack tension specimens. Failure assessment diagrams were generated and showed the fracture data close to the failure boundary. Fracture strength of any other cracked configurations can be evaluated from the present fracture criterion, by knowing the stress intensity equation.

References

[1] GOVINDAN POTTI P K, NAGESWARA RAO B, SRIVATSAVA V K. Residual strength of aluminum–lithium alloy center surface crack tension specimens at cryogenic temperatures [J]. Cryogenics, 2000, 40: 789−795.

[2] CHRISTOPHER T, SANKARANARAYANASAMY K, NAGESWARA RAO B. Fracture strength of flawed cylindrical pressure vessels under cryogenic temperatures [J]. International Journal of Cryogenics, 2002, 42: 661−673.

[3] CHRISTOPHER T, SANKARANARAYANASAMY K, NAGESWARA RAO B. Fracture behavior of maraging steel tensile specimens and pressurized cylindrical vessels [J]. Fatigue, Fracture of Engineering Materials & Structures, 2004, 27: 177−186.

[4] CHRISTOPHER T, SANKARANARAYANASAMY K, NAGESWARA RAO B. Failure assessment on tensile cracked specimens of aluminum alloys [J]. Trans ASME Journal of Pressure Vessels Technology, 2004, 126: 404−406.

[5] SIH G C. Handbook of stress intensity factors [M]. Pennsylvania: Lehigh University, 1973.

[6] WADDOUPS M E, EISENMAN J R, KAMINSKI B E. Macroscopic fracture mechanics of advanced composite materials [J]. Journal of Composite Materials, 1971, 5: 446−451.

[7] MURAKAMI Y. Stress intensity factors handbook [M]. New York: Pergamon Press, 1987.

[8] NEWMAN J C Jr, RAJU I S. Analysis of surface cracks under tension or bending loads [R]. NASA-TP-1578, 1979.

[9] NEWMAN J C Jr. Fracture analysis of surface and through cracks in cylindrical pressure vessels [R]. NASA-TND-8325, 1976.

2219-T87 铝合金的中心表面裂纹拉伸试样的断裂强度

S. RAJAKUMAR[1], T. CHRISTOPHER[2]

1. Thanthai Periyar Government Institute of Technology, Vellore-632002, India;

2. Government College of Engineering, Perumalpuram, Tirunelveli-627007, India

摘　要：将 2219-T87 铝合金板材进行低温拉伸试验，用改进的固有缺陷模型分析铝合金基材和焊接接头金属表面裂纹试样的断裂强度数据，通过构成的失效评估图来确定材料的断裂参数。通过考虑材料的极限拉伸强度、铝基材及焊接接头金属的断裂强度数据，对具有不同厚度的中心表面裂纹拉伸试样进行断裂分析。由拉伸断裂板材所得到的失效评估图能够应用到由相同材料构成的任何开裂组件的失效压力估计。

关键词：中心穿透裂纹；拉伸试样；失效评估图；断裂强度；固有缺陷模型；2219-T87 铝合金

(Edited by YANG Hua)